

Supporting Information

Temporal Characteristics of Brown Carbon over the Central Indo-Gangetic Plain

Rangu Satish^{*}, Puthukkadan Shamjad[#], Navaneeth Thamban[#], Sachchida Tripathi[#], Neeraj Rastogi^{*\$}

^{*}Geosciences Division, Physical Research Laboratory, Ahmedabad, India.

[#]Department of Civil Engineering and Centre for Environmental Science and Engineering, Indian Institute of Technology-Kanpur, Kanpur, India.

^{\$}Corresponding author E-mail: nrastogi@prl.res.in

Content:

Figures S1-S9 and detailed description of positive matrix factorization (PMF) analysis are given in the text.

Number of Pages: 11

Number of Figures: 9

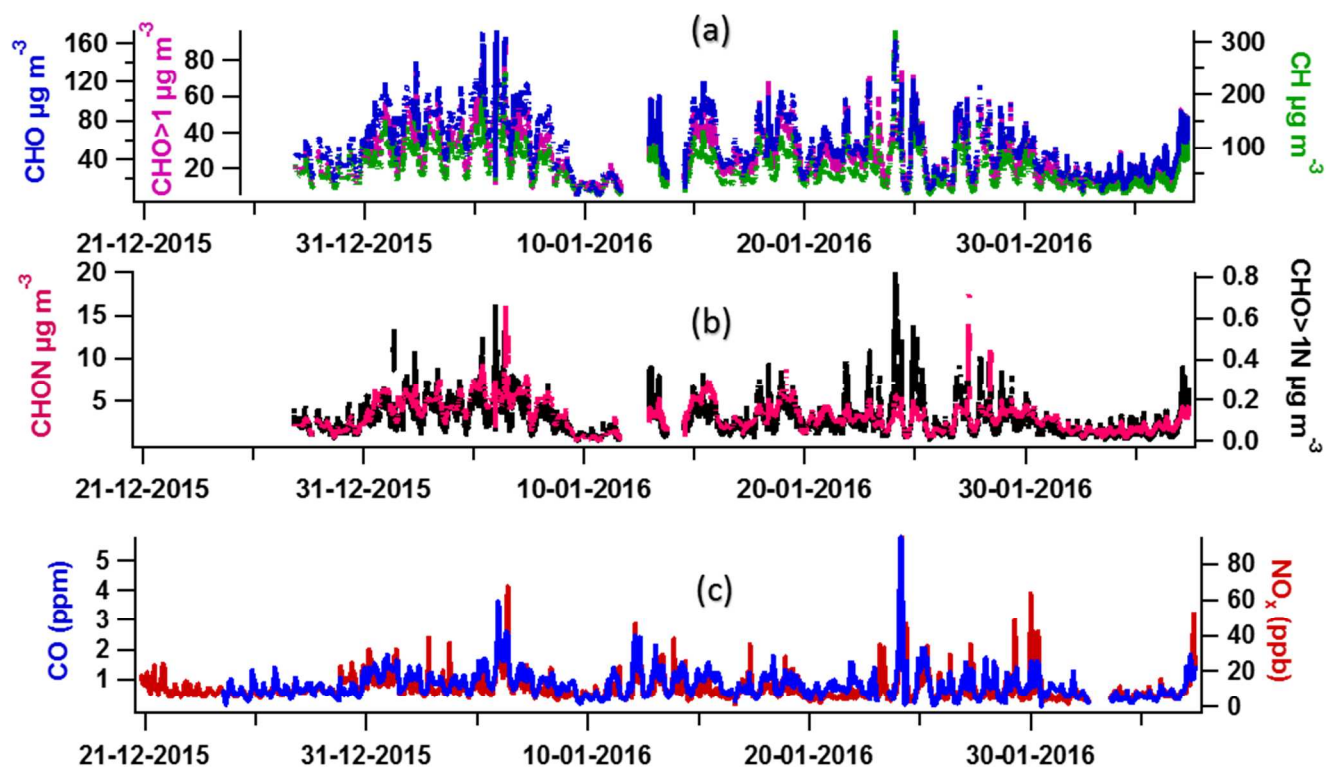
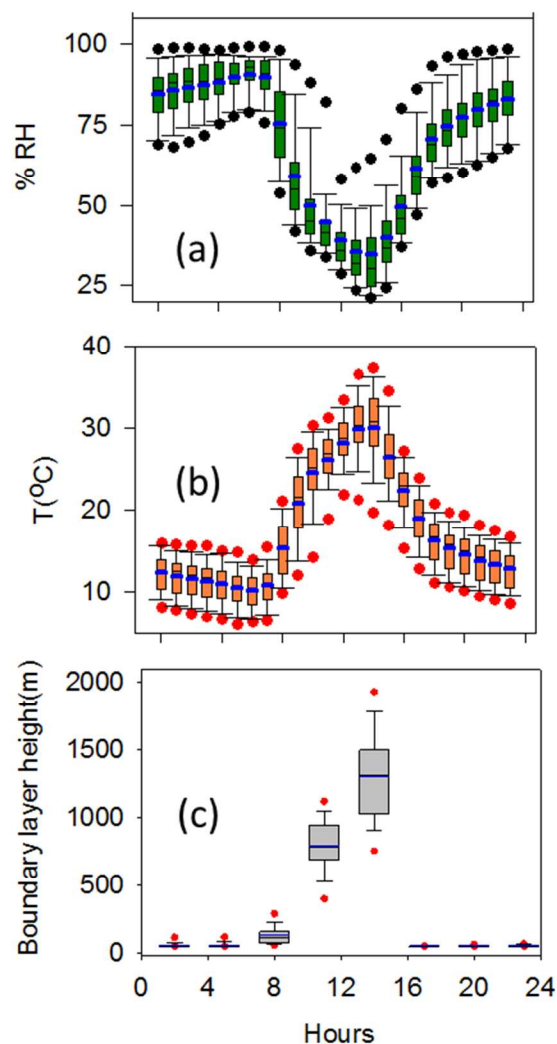


Fig. S1. Temporal variability in organic fragments (a): CH, CHO, CHO>1; (b): CHON, CHO>1N; (c): CO (ppm) and NO_x (ppb) during the study period.



29

30 Fig. S2: Box-whisker plot showing diurnal trends of (a) Relative humidity (%RH), (b)

31 Temperature (T, °C) and (c) atmospheric boundary layer height (m). The boundary layer height

32 (m) data (1 degree, 3 hourly, Global) was obtained from NOAA-Hysplit model. The boundary of

33 the box closest to zero indicates the 25th percentile, black and blue lines within the box represent

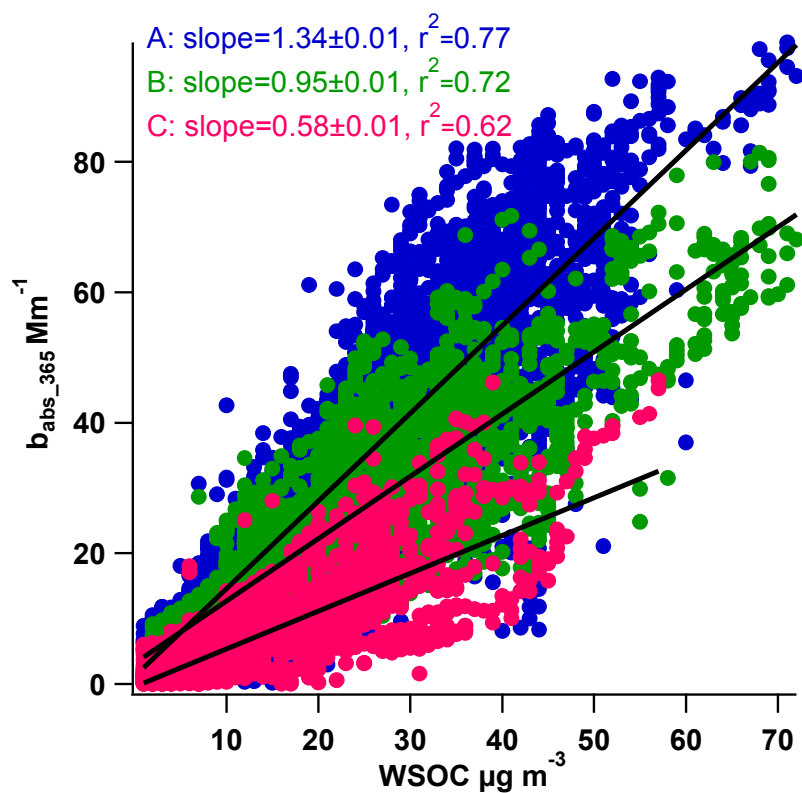
34 median and mean, respectively, and the boundary of the box farthest from zero indicates the 75th

35 percentile. Error bars above and below the box indicate the 90th and 10th percentiles. Red circles

36 are indicative of outliers.

37

38



39

40 Fig. S3: Scatter plot between the WSOC ($\mu\text{g m}^{-3}$) and b_{abs_365} (Mm^{-1}) at different periods of the
 41 day, where A: 18:00-06:00 hours (Evening + Night), B: 06:00-11:00 hours (Morning), and C:
 42 11:00-18:00 hours (Middle of the day), respectively.

43

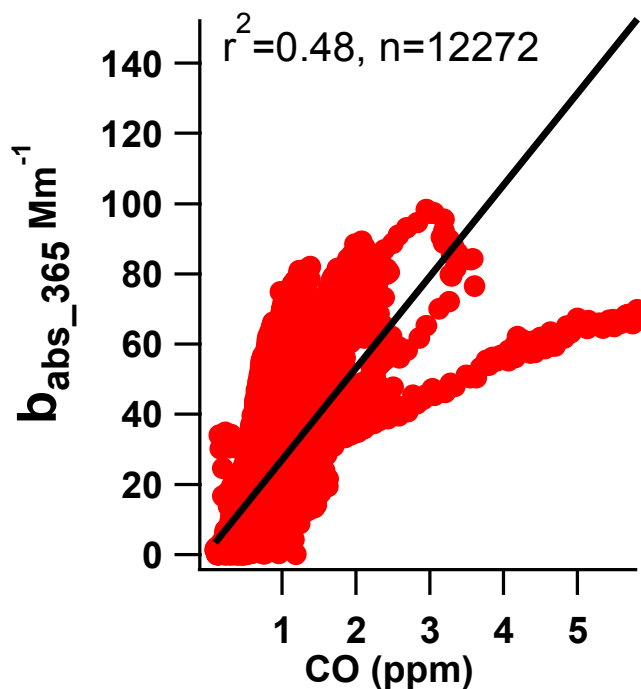


Fig. S4: Scatter plot between the b_{abs_365} (Mm^{-1}) and CO (ppm) during the study period.

Positive matrix factorization (PMF) analysis of organic aerosols (OA):

Positive matrix factorization (PMF) analysis¹ was performed on the V-mode high resolution (HR) organic mass spectra of AMS (m/z 12-120) for one to eight factors to find the optimal solution. In PMF, the observed data is defined as a bilinear factor model, which is solved with a least square fitting method. This fitting process reduces the sum of squares of the ratios between the fit residuals and error estimates at each data point². During PMF analysis, rotation values (fPeak) were varied from -5 to 5 with an interval of 0.5. Decrease in Q/Qexp values from 7.20 (4 factors) to 6.23 (8 factors) indicate that the additional factors explains more of the variation in the data³. An eight factor (fPeak=0) solution was selected based on this Q/Qexp

value of 6.23 (Fig S5b), the residuals (Fig. S5e), the physical interpretability (Fig. S6) and correlation with external factors (Fig. S7).

Details of PMF diagnostics are shown in the Figure S5. The correlation plot of PMF factors with organic (m/z 43, m/z 44, m/z 60), inorganic (SO_4^{2-} , NO_3^-) and external tracers (CO, BC) are shown in Fig. S7. The LVOOA-1 and LVOOA-2 factors were well correlated with AMS derived SO_4^{2-} ($r^2=0.71$) and m/z 44 i.e., CO_2^+ ($r^2=0.28$) respectively. The BBOA factor ($\text{O/C}=0.26$) was identified by its good correlation with m/z 60 i.e. $\text{C}_2\text{H}_4\text{O}_2^+$ ($r^2=0.83$), a well-established levoglucosan fragment⁴⁻⁶. SVOOA-BBOA-1 ($\text{O/C}=0.55$, more oxygenated) and SVOOA-BBOA-2 ($\text{O/C}=0.43$, less oxygenated) were correlated well with m/z 43 i.e., $\text{C}_2\text{H}_3\text{O}^+$ ($r^2=0.57$ and 0.45 , respectively), NO_3^- ($r^2=0.48$ and 0.43 respectively) and with BBOA tracer i.e., m/z 60 ($\text{C}_2\text{H}_4\text{O}_2^+$) ($r^2=0.56$ and 0.30 , respectively). This positive correlation of SVOOA-BBOA factors with NO_3^- and m/z 43 indicated the semi volatile characteristics of these factors and their moderate correlation with m/z 60 shown that they had significant contribution from biomass burning emissions. Primary organic aerosol factor HOA was correlated with aethalometer derived BC concentrations (at 880 nm) and carbon monoxide (CO) concentration derived from gas analyzer (Serinus, Ecotech). The strong positive correlation of HOA with these external factors i.e. BC and CO ($r^2=0.71$, 0.77 respectively) indicated that HOA was linked with combustion related sources.

The final source profiles of PMF factors are presented in Fig. S6. These factors include four low volatile oxygenated organic aerosol factors (LVOOA-1a, LVOOA-1b, LVOOA-1c, LVOOA-2), two semi volatile oxygenated organic aerosol factors those also have significant contribution from biomass burning organics (SVOOA-BBOA-1, SVOOA-BBOA-2), one hydrocarbon like organic aerosols (HOA), and one biomass burning organic aerosol (BBOA).

Here, LVOOA-1a, LVOOA-1b, LVOOA-1c were combined and merged into a single factor LVOOA-1, as the correlation coefficients (r^2) between factor profiles of LVOOA-1a (O/C=0.64), LVOOA-1b (O/C=0.67), LVOOA-1c (O/C=0.54) were more than 0.90 and have similar O/C values. The LVOOA 1 (O/C=0.62) was less oxygenated as compared to LVOOA-2 (O/C=0.94). The SVOOA-BBOA-1 (O/C=0.55) was more oxygenated as compared to SVOOA-BBOA-2 (O/C=0.43). Primary organic aerosol (POA) factors were identified as hydrocarbon like organic aerosol (HOA) and biomass burning organic aerosol (BBOA).

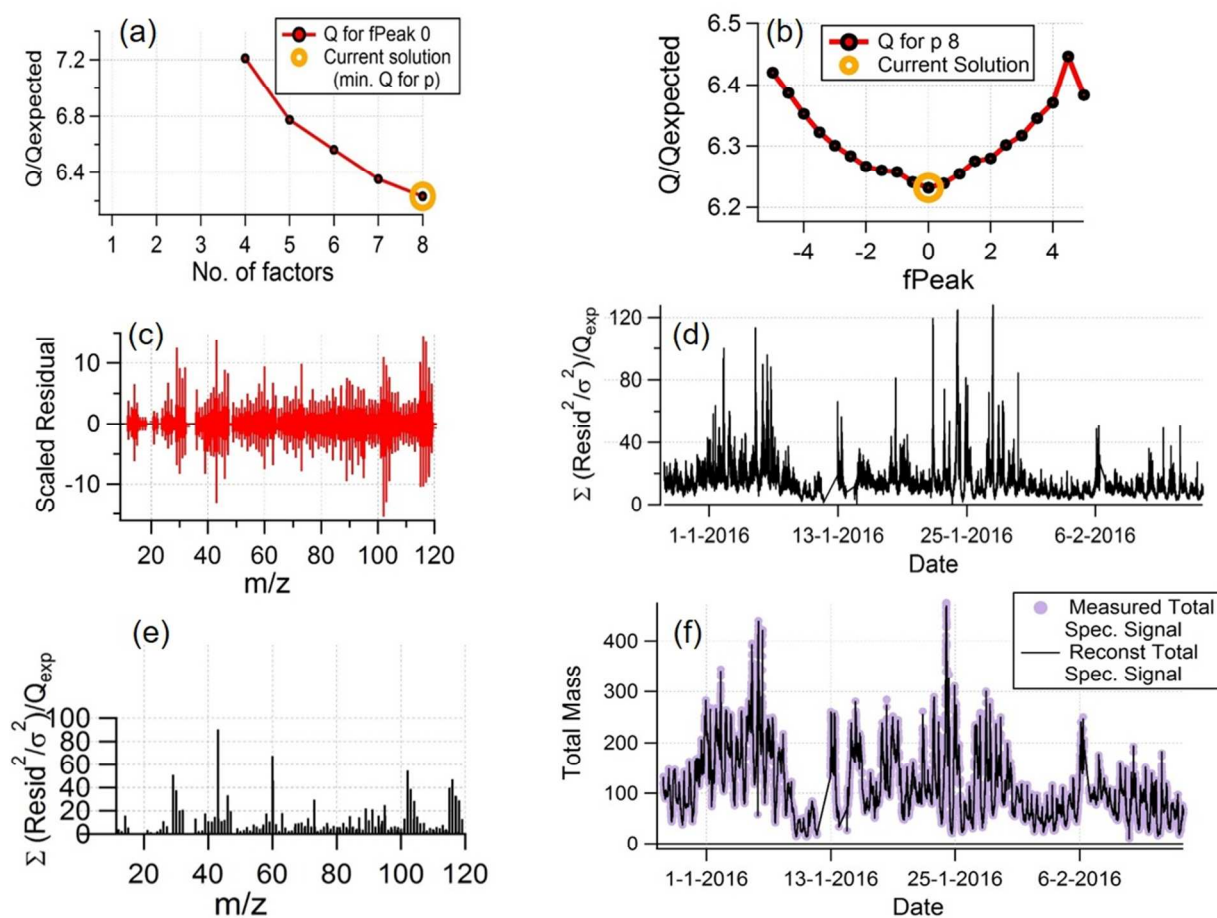


Fig. S5: Details of the PMF analysis and selection of optimum factors

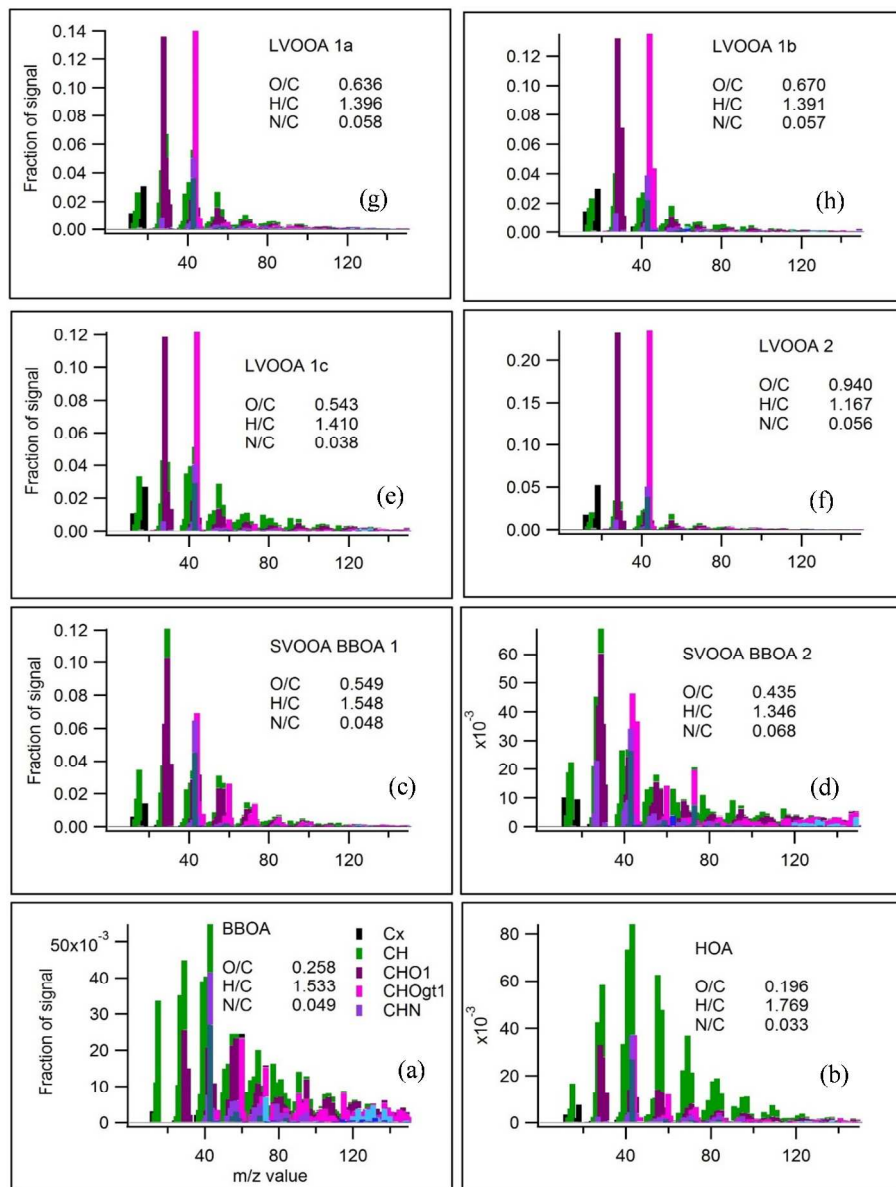
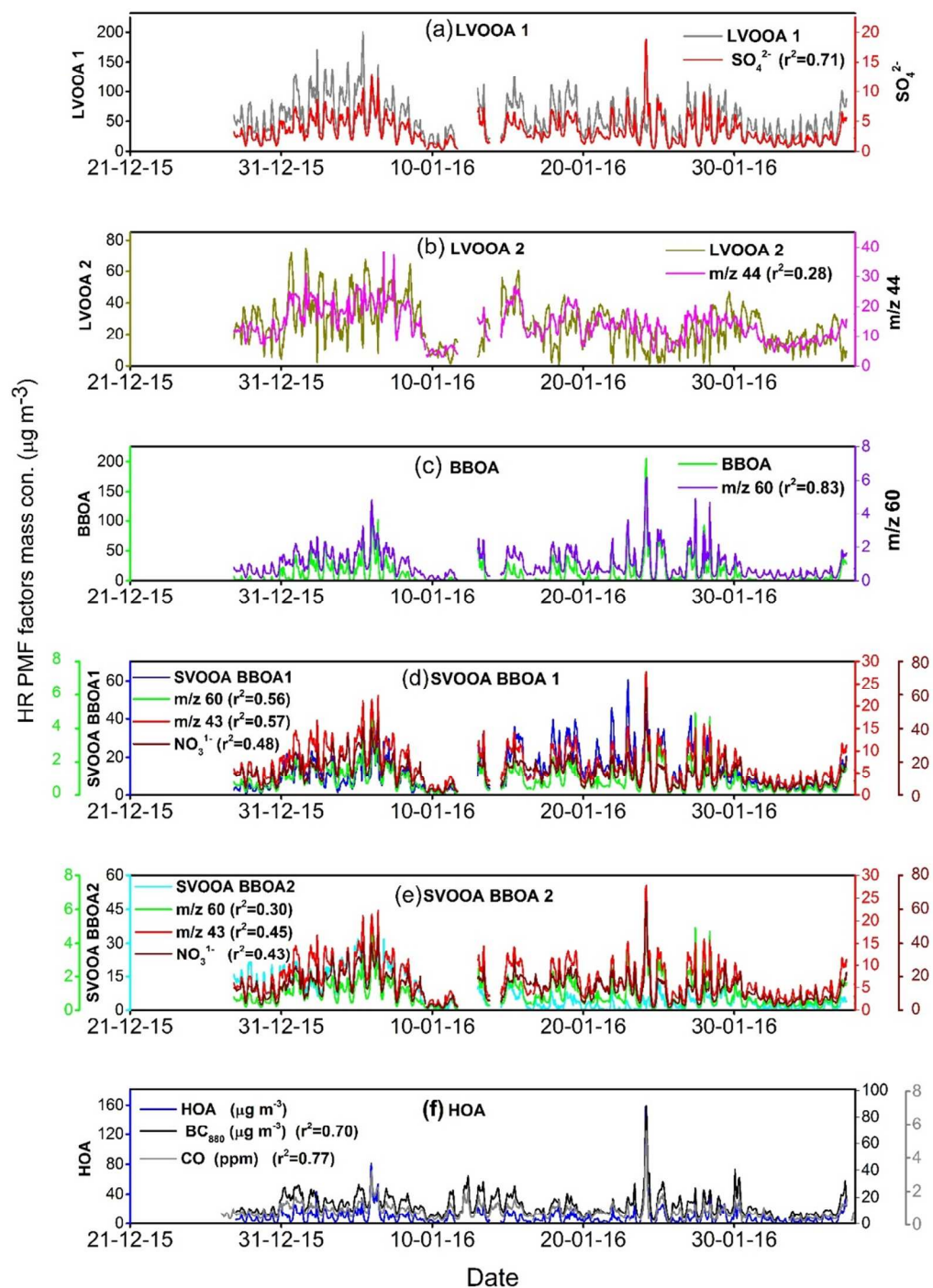


Fig. S6: Combined HR-PMF factor profiles. (a) biomass burning OA (BBOA), (b) hydrocarbon-like OA (HOA), (c) semi volatile oxygenated OA biomass burning OA 1 (SVOOA BOOA 1), (d) semi volatile oxygenated OA biomass burning OA 2 (SVOOA BOOA 2), (e) low volatile oxidized OA 1c (LVOOA 1c), (f) low volatile oxidized OA 2 (LVOOA 2), (g) low volatile oxidized OA 1a (LVOOA 1a), (h) low volatile oxidized OA 1b (LVOOA 1b).



99 Fig. S7: Correlation of PMF factors (LVOOA 1, LVOOA 2, BBOA, SVOOA BBOA 1, SVOOA
100 BBOA 2, HOA) with various tracers.

Diurnal variability of PMF factors and meteorological parameters:

Total OA concentration peaks in the morning hours (08:00 to 10:00) due to active primary emissions from vehicles and bio-fuel burning, and photochemical SOA formation whereas, peak during late evening/night hours (18:00 to 23:00) is attributable predominantly to primary emission. Similar diurnal trends were observed for BBOA, SVOOA-BBOA-1, SVOOA-BBOA-2, HOA, LVOOA-1, but different trend was observed for LVOOA-2 (aged/highly oxygenated OA). LVOOA-1 factor contain highest mass fraction of OA among all other factors and its O/C and H/C ratios suggests that this fraction could be from both primary and secondary sources. Both BBOA and HOA follow the similar trends as that of total OA but, during daytime (12:00 to 17:00) the concentrations were reduced by up to ~80% due to absence of primary sources, and when atmospheric boundary layer height is at its maximum.

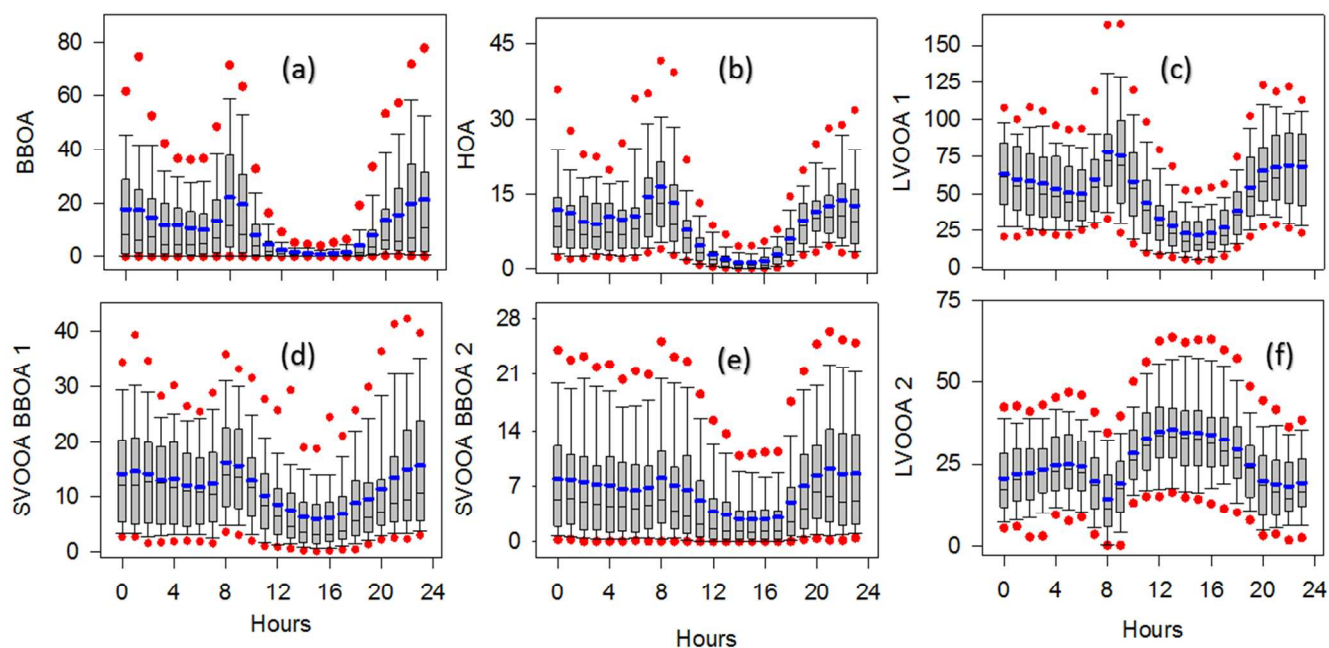


Fig. S8: Box-whisker plot showing diurnal trends of OA as well as its HR-PMF derived factors (HOA, BBOA, SVOOA BBOA 1, SVOOA BBOA 2, LVOOA 1, LVOOA 2 in $\mu\text{g m}^{-3}$). For details of lines, bars and symbols, refer to caption of Fig. 3.

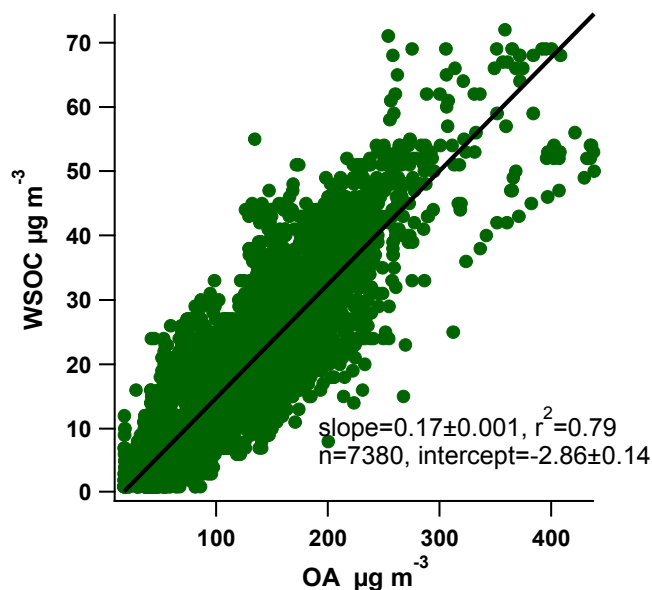


Fig. S9: Scatter plot between the WSOC ($\mu\text{g m}^{-3}$) and OA ($\mu\text{g m}^{-3}$) during the study period.

References:

- (1) Paatero, P.; Tapper, U. Positive matrix factorization: A non-negative factor model with optimal utilization of error estimates of data values. *Environmetrics* **1994**, 5 (2), 111–126.
- (2) He, L. Y.; Huang, X. F.; Xue, L.; Hu, M.; Lin, Y.; Zheng, J.; Zhang, R.; Zhang, Y. H. Submicron aerosol analysis and organic source apportionment in an urban atmosphere in Pearl River Delta of China using high-resolution aerosol mass spectrometry. *J. Geophys. Res. Atmos.* **2011**, 116 (12), 1–15.
- (3) Ulbrich, I. M.; Canagaratna, M. R.; Zhang, Q.; Worsnop, D. R.; Jimenez, J. L. Interpretation of organic components from Positive Matrix Factorization of aerosol mass spectrometric data. *Atmos. Chem. Phys. Atmos. Chem. Phys.* **2009**, 9, 2891–2918.
- (4) Alfarra, M. R.; Prevot, A. S. H.; Szidat, S.; Sandradewi, J.; Weimer, S.; Lanz, V. A.; Schreiber, D.; Mohr, M.; Baltensperger, U. Identification of the mass spectral signature of organic aerosols from wood burning emissions. *Environ. Sci. Technol.* **2007**, 41 (16), 5770–5777.
- (5) Mohr, C.; Huffman, J. A.; Cubison, M. J.; Aiken, A. C.; Docherty, K. S.; Kimmel, J. R.; Ulbrich, I. M.; Hannigan, M.; Jimenez, J. L. Characterization of Primary Organic Aerosol Emissions from Meat Cooking, Trash Burning, and Motor Vehicles with High-Resolution Aerosol Mass Spectrometry and Comparison with Ambient and Chamber Observations. *Environ. Sci. Technol.* **2009**, 43 (7), 2443–2449.
- (6) Weimer, S.; Alfarra, M. R.; Schreiber, D.; Mohr, M.; Prévôt, A. S. H.; Baltensperger, U. Organic aerosol mass spectral signatures from wood-burning emissions: Influence of burning conditions and wood type. *J. Geophys. Res.* **2008**, 113 (D10), D10304.